per junction. Although 29,689 junctions in HEK and 24,848 in B cells had only one read, those were considered highly notable, as we expect at most 23 reads hitting a junction by chance in the entire data set (16). Splice junctions were associated with 81% of the expressed genes. We also observed splice junctions for ~260 genes in each cell line that were not classified as expressed (Tables 1 and 2). Of those, 70% had between 1 and 4 reads and 30% were silent, suggesting a very low activity. The fact that 2275 expressed genes in HEK and 2013 in B cells had no splice-junction reads correlated with the fact that those genes contained fewer exons and a lower activity than the average, reducing the probability to hit a splice junction.

We observed 95% of the splicing events expected in this data set, given the current sequencing depth (Table 1) (16). We identified 4096 previously unknown splice junctions in 3106 genes, mostly called by single reads and unique to one cell type (Table 1). Many of these junctions were associated with actively transcribed genes exhibiting more exons than average, pointing to rare splicing events. Approximately 6% of all splice-junction reads identified AS events (6416 junctions in 3916 genes HEK and 5195 junctions in 3262 genes in B cells) (table S9). In a parallel study surveying the mouse transcriptome, AS forms were observed for 3462 genes in three tissues (28), but no attempts were made to search for previously unrecognized junctions. Within a cell type, junction reads identify AS in 30% of the expressed genes, where exon skipping was largely overrepresented (Fig. 3A). Skipping events affected mostly one or two exons, with a sharp

decline between one and five exons (Fig. 3B). An illustrative example of AS is given for PKM2, also showing that the read density reflects the exon usage (Fig. 3C). Very complex patterns of AS could be detected. For instance, with the use of EIF4G1 coding for the eukaryotic translation initiation factor 4 gamma 1, we showed 12 AS junctions in B cells, of which five have not yet been identified (fig. S3). Although AS is known to regulate the expression of EIF4G1 (29, 30), such a complex pattern had never been described before.

References and Notes

1. H. Lehrach et al., in Genome Analysis: Genetic and Physical Mapping, vol. 1, K. Davies, Ed. (Cold Spring Harbor Laboratory Press, Cold Spring Harbor, NY, 1990), pp. 39–81.
2. G. G. Lennon, H. Lehrach, Trends Genet. 7, 314 (1991).
3. E. M. Southern, Curr. Opin. Genet. Dev. 2, 412 (1992).
4. G. M. Hampton, H. F. Frierson, Trends Mol. Med. 9, 5 (2003).
5. T. R. Hughes et al., Cell 102, 109 (2000).
6. P. Bertone et al., Science 306, 2242 (2004), published online 11 November 2004; 10.1126/science.1103388.
7. J. Cheng et al., Science 308, 1149 (2005), published online 24 March 2005; 10.1126/science.1108625.
8. Q. Pan et al., Mol. Cell 16, 929 (2004).
9. J. A. Calarco, A. L. Saltzman, J. Y. Ip, B. J. Blencowe, Adv. Exp. Med. Biol. 623, 64 (2007).
10. V. E. Velculescu, L. Zhang, B. Vogelstein, K. W. Kinzler, Science 270, 484 (1995).
11. C. V. Jongeneel et al., Proc. Natl. Acad. Sci. U.S.A. 100, 4702 (2003).
12. J. B. Kim et al., Science 316, 1481 (2007).
13. U. Nagalakshmi et al., Science 320, 1344 (2008), published online 30 April 2008; 10.1126/science.1158441.
14. R. Lister et al., Cell 133, 523 (2008).
15. B. T. Wilhelm et al., Nature 453, 1239 (2008).
16. Materials and methods are available as supporting material on Science Online.
17. T. J. Hubbard et al., Nucleic Acids Res. 35, D610 (2007).
18. A. S. Brodsky et al., Genome Biol. 6, R64 (2005).
19. A. Barski et al., Cell 129, 823 (2007).
20. T. Margaritis, F. C. Holstege, Cell 133, 581 (2008).
21. T. Shiraki et al., Proc. Natl. Acad. Sci. U.S.A. 100, 15776 (2003).
22. J.-P. Z. Wang, B. G. Lindsay, J. Am. Stat. Assoc. 100, 942 (2005).
23. F. Liu et al., BMC Genomics 8, 153 (2007).
24. M. Barnes, J. Freudenberg, S. Thompson, B. Aronow, P. Pavlidis, Nucleic Acids Res. 33, 5914 (2005).
25. C. V. Jongeneel et al., Genome Res. 15, 1007 (2005).
26. L. Shi et al., Nat. Biotechnol. 24, 1151 (2006).
27. S. F. Altschul, W. Gish, W. Miller, E. W. Myers, D. J. Lipman, J. Mol. Biol. 215, 403 (1990).
28. A. Mortazavi, B. A. Williams, K. McCue, L. Schaeffer, B. Wold, Nat. Methods 5, 621 (2008).
29. M. P. Byrd, M. Zamora, R. E. Lloyd, J. Biol. Chem. 280, 18610 (2005).
30. M. J. Coldwell, S. J. Morley, Mol. Cell. Biol. 26, 8448 (2006).
31. The Gene Expression Omnibus accession number for the microarrays and sequence data is GSE11892. Data are displayed in a public version of browser interfaces developed by the Max Planck Institute for Molecular Genetics (http://promotion.molgen.mpg.de/cgi-bin/gbrowse/Hs.Solexa) and Genomatix (www.genomatix.de/MPI). This work was supported in part by the Max Planck Society, the European Union [AnEUploidy (LSHG-CT-2006-037627) and BioSapiens (LHSG-CT-2003-503265)], the National Genome Research Network, and the Federal Ministry for Education and Research of Germany [BioChancePLUS-3 (0313724A) to A.K. and M.S.].

Small CRISPR RNAs Guide Antiviral Defense in Prokaryotes

Stan J. J. Brouns,[1]* Matthijs M. Jore,[1]* Magnus Lundgren,[1] Edze R. Westra,[1] Rik J. H. Slijkhuis,[1] Ambrosius P. L. Snijders,[2] Mark J. Dickman,[2] Kira S. Makarova,[3] Eugene V. Koonin,[3] John van der Oost[1]†

Prokaryotes acquire virus resistance by integrating short fragments of viral nucleic acid into clusters of regularly interspaced short palindromic repeats (CRISPRs). Here we show how virus-derived sequences contained in CRISPRs are used by CRISPR-associated (Cas) proteins from the host to mediate an antiviral response that counteracts infection. After transcription of the CRISPR, a complex of Cas proteins termed Cascade cleaves a CRISPR RNA precursor in each repeat and retains the cleavage products containing the virus-derived sequence. Assisted by the helicase Cas3, these mature CRISPR RNAs then serve as small guide RNAs that enable Cascade to interfere with virus proliferation. Our results demonstrate that the formation of mature guide RNAs by the CRISPR RNA endonuclease subunit of Cascade is a mechanistic requirement for antiviral defense.

The clusters of regularly interspaced short palindromic repeat (CRISPR)–based defense system protects many bacteria and archaea against invading conjugative plasmids, transposable elements, and viruses (1–8). Resistance is acquired by incorporating short stretches of invading DNA sequences in genomic CRISPR loci (1, 9, 10). These integrated sequences are thought to function as a genetic memory that prevents the host from being infected by viruses containing this recognition sequence. A number of CRISPR-associated (cas) genes (11–13) has been reported to be essential for the phage-resistant phenotype (1). However, the molecular mechanism of this adaptive and inheritable defense system in prokaryotes has remained unknown.

The Escherichia coli K12 CRISPR/cas system comprises eight cas genes: cas3 (predicted HD-nuclease fused to a DEAD-box helicase), five genes designated casABCDE, cas1 (predicted integrase) (13), and the endoribonuclease gene cas2 (14) (Fig. 1A and table S1). In separate experiments, each Cas protein was tagged at both the N and C terminus and produced along with the complete set of untagged Cas proteins (15). Affinity purification of the tagged component enabled the identification of a protein complex composed of five Cas proteins: CasA, CasB, CasC, CasD, and CasE (Fig. 1B). The

[1]Laboratory of Microbiology, Department of Agrotechnology and Food Sciences, Wageningen University, Dreijenplein 10, 6703 HB Wageningen, Netherlands. [2]Biological and Environmental Systems, Department of Chemical and Process Engineering, University of Sheffield, Mappin Street, Sheffield S1 3JD, UK. [3]National Center for Biotechnology Information, National Library of Medicine, NIH, Bethesda, MD 20894, USA.

*These authors contributed equally to this work.
†To whom correspondence should be addressed. E-mail: john.vanderoost@wur.nl

complex, denoted Cascade (CRISPR-associated complex for antiviral defense), could be isolated from *E. coli* lysates using any of the tagged subunits of the complex as bait, except for CasA.

The function of Cascade was studied by analyzing the effect of in-frame *cas* gene knockouts (*16*) on the formation of transcripts of the CRISPR region in *E. coli* K12 (Fig. 1A). Northern analysis of total RNA with single-stranded spacer sequences as a probe showed transcription of the CRISPR region in the direction downstream of the *cas2* gene (Figs. 1A and 2A) and no transcription in the opposite direction. Analysis of control strains (wild type and a non-*cas* gene knockout) revealed a small CRISPR-RNA (crRNA) product of ~57 nucleotides (Fig. 2A). The same product was present in much higher amounts in the *casA*, *casB*, and *casC* knockout strains but absent from strains lacking the overlapping genes *casD* and *casE* (Fig. 2A). The small crRNAs seem to be cleaved from a multiunit crRNA precursor (pre-crRNA) (*7, 17, 18*), as is evident from the presence of two and three repeat-spacer units (~120 and ~180 nucleotides) that show up in the ΔcasA, ΔcasB, and ΔcasC strains (Fig. 2A). The ΔcasE strain contained a large pre-crRNA, suggesting that the disruption of this gene prevents pre-crRNA cleavage.

To study the accumulation and cleavage patterns of crRNAs in the *E. coli* K12 knockout strains in more detail and to rule out any effects of the gene disruptions on the expression of downstream or upstream *cas* genes, the five subunits of Cascade and the K12-type pre-crRNA were expressed in *E. coli* BL21(DE3), which lacks endogenous *cas* genes (*19*). Northern analysis showed that crRNAs of ~57 nucleotides were only produced in strains containing the Cascade complex (Fig. 2B). By omitting the individual subunits one by one, it became apparent that the small crRNA was absent only in the strain that lacked *casE* (Fig. 2B), indicating that this is the only Cascade subunit essential for pre-crRNA cleavage.

Activity assays with purified Cascade showed that the complex is capable of cleaving the *E. coli* K12 pre-crRNA into fragments of ~57 nucleotides in vitro (Fig. 2C). However, no cleavage was observed with either pre-crRNA from *E. coli* UTI89, which contains repeats with a different sequence (*20*), or a non-crRNA template (Fig. 2C). The RNA cleavage reaction proceeded in the absence of divalent metal ions and adenosine triphosphate and reached saturation level within 5 min. To investigate whether the CasE subunit is sufficient for pre-crRNA cleavage activity, it was overproduced as a fusion with the *E. coli* maltose binding protein (MalE). Like the complete Cascade, the CasE fusion protein cleaved only the K12-type pre-crRNA (Fig. 2D), showing that CasE is an unusual endoribonuclease that does not require the other Cascade subunits. We cannot rule out the possibility that pre-crRNA cleavage is an autocatalytic, ribozyme-like reaction, in which CasE is an essential RNA chaperone.

CasE belongs to one of the numerous families of repeat-associated mysterious proteins, the largest and most diverse class of Cas proteins (*12, 13*). The crystal structure of a CasE homolog from *Thermus thermophilus* HB8 shows that the protein contains two domains with a ferredoxin-like fold, and displays overall structural similarity to a variety of RNA-binding proteins (*13, 21*). On the basis of structure and amino acid conservation analysis of this protein family (fig. S1), the invariant residue His[20] was mutated to Ala to analyze the effect on pre-crRNA cleavage. Northern blots indicated that crRNAs of ~57 nucleotides were no longer formed in the strain containing Cascade-CasE[H20A] (Fig. 2E). Moreover, although the mutated CasE was still incorporated into Cascade, the pre-crRNA cleaving ability of purified Cascade was abolished (Fig. 2F), providing further support for the essential role of CasE in pre-crRNA cleavage and suggesting that the conserved His residue is involved in catalysis.

The crRNA cleavage sites were examined by simultaneous expression of K12-type pre-crRNA and Cascade. Under these conditions, the purification of Cascade yielded substantial amounts of copurified RNAs of ~57 nucleotides (Fig. 3A). Cloning and sequencing of this Cascade-bound RNA revealed that 85% of the clones [67 out of 79 clones (67/79)] were derived from crRNAs, of which 78% (52/67) started with the last eight bases of the repeat sequence (AUAAACCG) (Fig. 3B and fig. S2). This well-defined 5' end

Fig. 1. The composition of the Cascade complex. (**A**) Schematic diagram of the CRISPR/*cas* gene cluster of *E. coli* K12 W3110. Repeats and spacers are indicated by diamonds and rectangles, respectively. A palindrome in the repeat is marked by convergently pointing arrows. Protein family nomenclature is as described in (*11, 12*). (**B**) Coomassie blue–stained SDS-polyacrylamide gel of the affinity purified protein complex using either the N-terminal StrepII-tag (S) or C-terminal His-tag (H) of each of the subunits CasB, CasC, CasD, or CasE as bait. Asterisks indicate the 5.5 kD larger double-tagged subunits. Marker sizes in kilodaltons on the left; location of untagged subunits on the right.
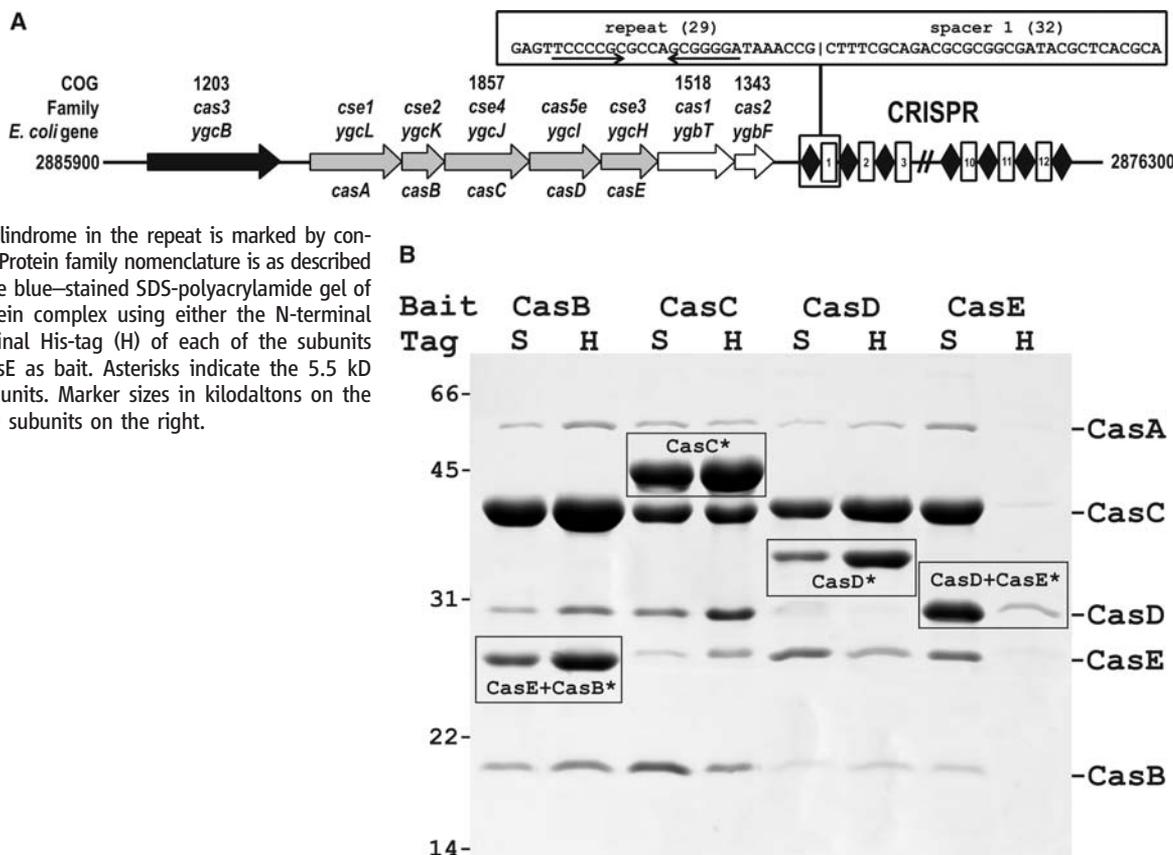
Fig. 2. Cascade cleaves CRISPR RNA precursors into small RNAs of ~57 nucleotides (marked by arrows). (**A**) Northern analysis of total RNA of WT *E. coli* K12 (WT), a non-*cas* gene knockout (Δ*u*, *uidA*, β-glucuronidase), and Cascade gene knockouts using the single-stranded spacer sequence BG2349 (table S2) as a probe. (**B**) Northern blot as in (A) of total RNA from *E. coli* BL21 (DE3) expressing the *E. coli* K12 pre-crRNA and either the complete or incomplete Cascade complex. (**C**) Activity assays with purified Cascade using in vitro transcribed α-^{32}P–uridine triphosphate–labeled pre-crRNA from *E. coli* K12 (repeat sequence: GAGU-UCCCCGCCAGCGGGGA-UAAACCG), *E. coli* UTI89 (repeat sequence: GUUCA-CUGCCGUACAGGCAGCU-UAGAAA), and non-crRNA as substrates. (**D**) Activity assays as shown in (C) for 15 min with purified MalE-LacZα and MalE-CasE fusion proteins. (**E**) Northern blot as shown in (B) with Cascade or Cascade-CasE^{H20A}. (**F**) Activity assays as shown in (C) for 30 min with purified Cascade or Cascade-CasE^{H20A}.
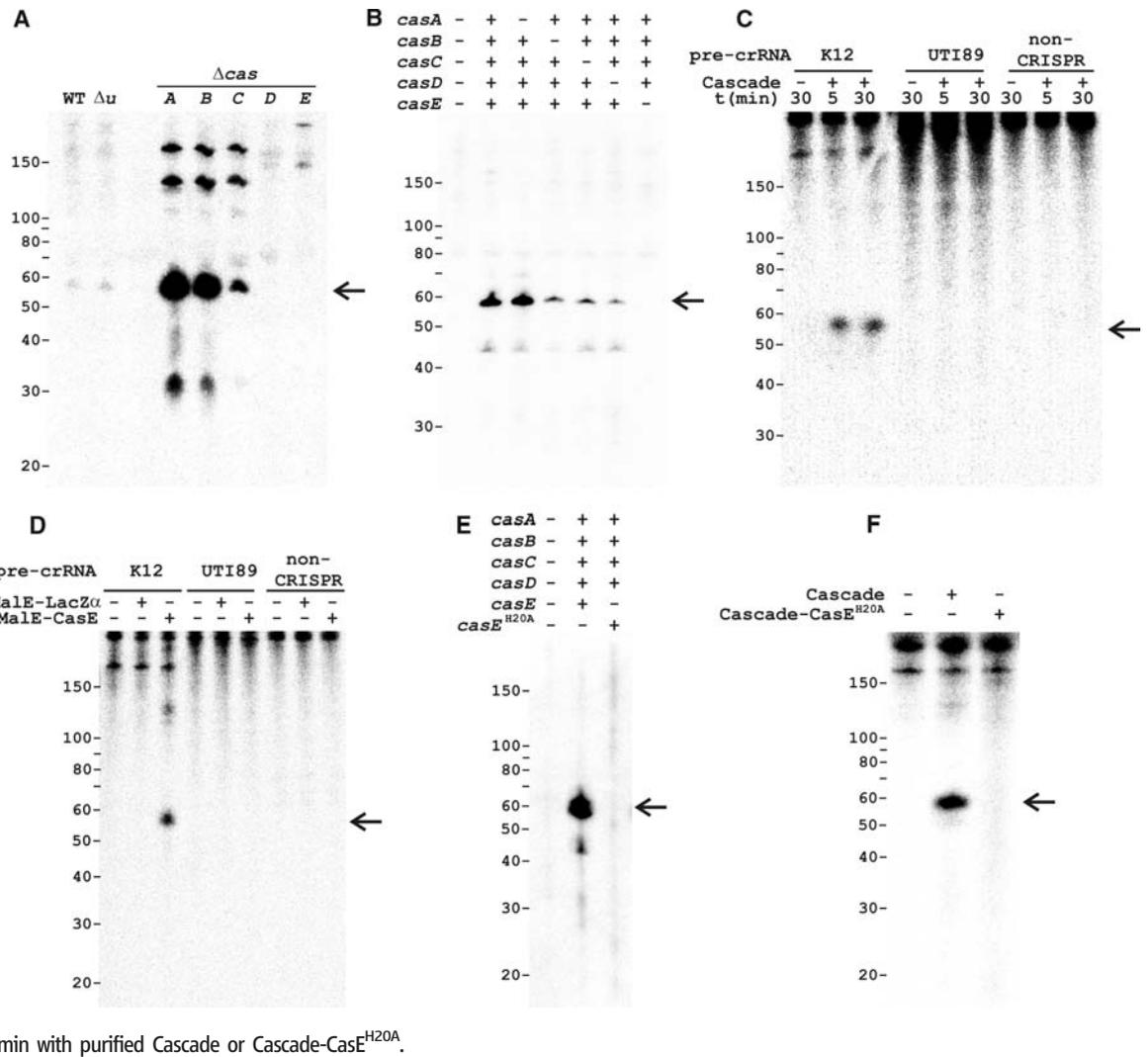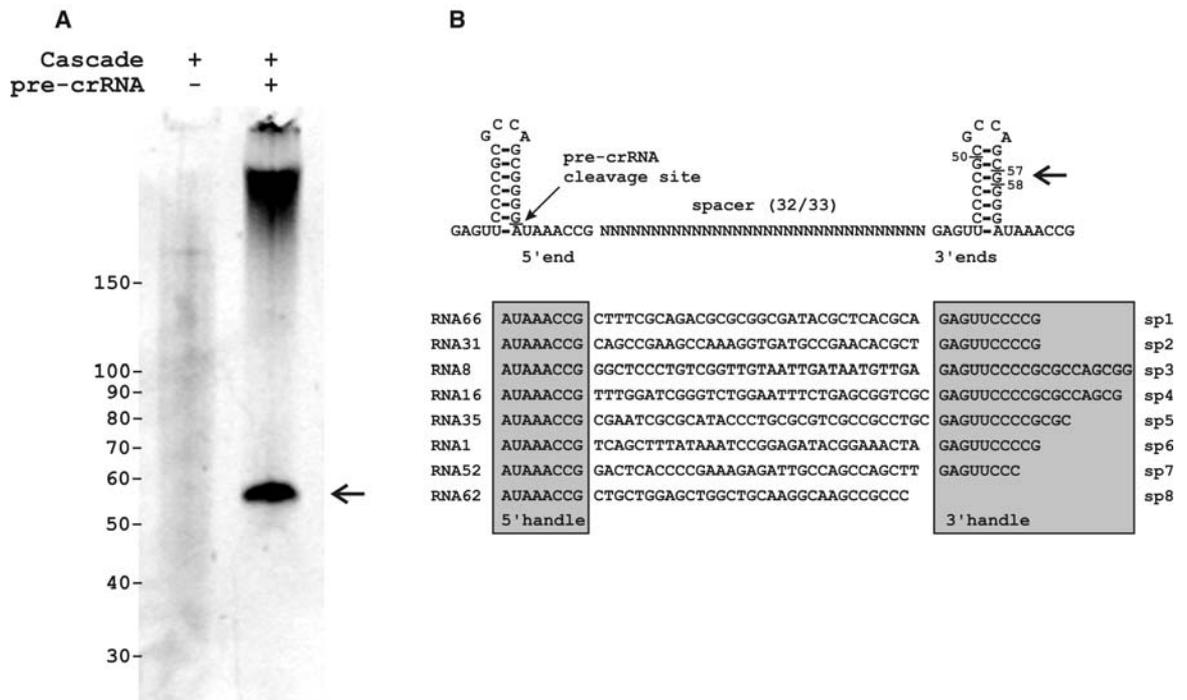
Fig. 3. Cleaved crRNAs remain bound by Cascade. (**A**) Denaturing polyacrylamide gel showing the crRNA (marked by the arrow) isolated from purified Cascade in the absence and presence of co-expressed pre-crRNA. (**B**) Secondary structure of pre-crRNA repeats and example sequences of cloned crRNAs indicating the PCS and crRNA handles.

was followed by a complete spacer sequence and a less well-defined 3′ sequence ending in the next repeat region. A transcript of a single palindromic repeat can fold as a stable stem-loop of seven base pairs, which may facilitate recognition by RNA-binding Cas proteins ([8, 20]), such as CasE. The pre-crRNA cleavage site (PCS) appeared to be located immediately upstream of the 3′ terminal base of the stem-loop formed by the repeat (Fig. 3B). The clone library did not contain crRNAs of 61 nucleotides, which would be the result of a single endonuclease cleavage event in each repeat, given the size of a repeat (29 nucleotides) and most spacers (32 nucleotides). Instead, in agreement with experimental observations (Figs. 2 and 3A), the crRNAs were truncated at the 3′ end by at least two guanosine bases from the endonuclease cleavage site, removing several stem-forming bases.

To test whether crRNA-loaded Cascade gives rise to phage resistance, two artificial CRISPRs were designed against phage Lambda (λ). Each of these CRISPRs targeted four essential λ genes (fig. S3). The coding CRISPR (C_{1-4}) produced crRNAs complementary to both the mRNA and the coding strand of these four genes, whereas

the template CRISPR (T_{1-4}) targeted only the template strand of the same proto-spacer regions (fig. S3). A nontargeting CRISPR containing wild-type (WT) spacers with no similarity to the phage genome served as a control. Plaque assays with *E. coli* showed that the introduction of either one of these anti-λ phage CRISPRs in a strain expressing only Cascade did not result in reduced sensitivity of the host to a virulent Lambda phage (λ_{vir}) (Fig. 4A). However, strains that expressed Cascade and Cas3 were much less sensitive to phage infection. The template CRISPR rendered the strain insensitive to the phage at the highest phage titer tested ($>10^7$-fold less sensitive than the control strain), whereas the coding CRISPR reduced the sensitivity 10^2-fold (Fig. 4A) and produced plaques with a diameter $\sim 1/10$ of the standard λ plaque. The phage resistance phenotype was lost when Cascade was omitted (Fig. 4A), proving that both Cascade and Cas3 are required in this process. Moreover, strains containing Cas3 and Cascade-CasE^{H20A} displayed a sensitive phenotype, which shows that pre-crRNA cleavage is mechanistically required for phage resistance. The co-expression of Cas1 and Cas2 had no effect on the sensitivity

profile of the strain (Fig. 4A), suggesting that these proteins are involved in other stages of the CRISPR/*cas* mechanism. Plaque assays with single anti-λ spacers (fig. S3) showed that the total reduction of sensitivity observed with the four anti-λ spacers (C_{1-4} and T_{1-4}) (Fig. 4A) results from a synergistic effect of the individual spacers (C_1 to T_4) (Fig. 4B).

Our results demonstrate that a complex of five Cas proteins is responsible for the maturation of pre-crRNA to small crRNAs that are critical for mediating an antiviral response. These mature crRNAs contain the antiviral spacer unit flanked by short RNA sequences derived from the repeat on either side termed the 5′ and 3′ handle, which may serve as conserved binding sites for Cascade subunits, as has been suggested previously ([20]). The Cascade-bound crRNA serves as a guide to direct the complex to viral nucleic acids to mediate an antiviral response. We hypothesize that crRNAs target virus DNA, because anti-λ CRISPRs of both polarities lead to a reduction of sensitivity to the phage. The model is supported by previous observations that virus-derived sequences are integrated into CRISPR loci, irrespective of their orientation in the virus genome ([1–4, 7, 9, 10, 13]). We conclude that the transcription of CRISPR regions—and the cleavage of pre-crRNA to mature crRNAs by Cas proteins—is the molecular basis of the antiviral defense stage of the CRISPR/*cas* system, which enables prokaryotes to effectively prevent phage predation.
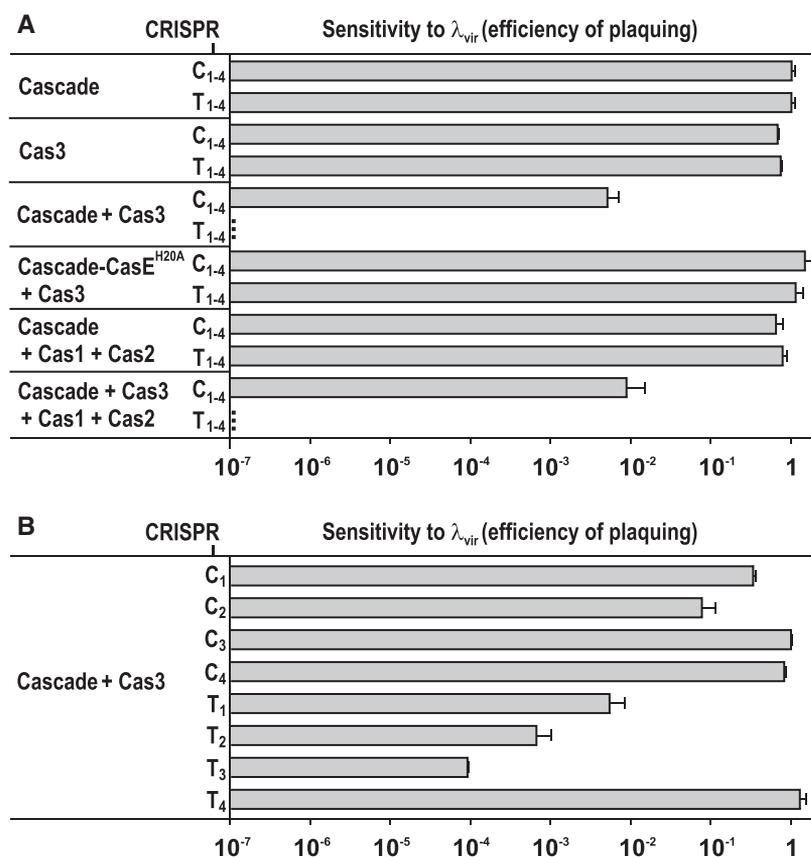
References and Notes

1. R. Barrangou *et al.*, *Science* **315**, 1709 (2007).
2. F. J. Mojica, C. Diez-Villasenor, J. Garcia-Martinez, E. Soria, *J. Mol. Evol.* **60**, 174 (2005).
3. C. Pourcel, G. Salvignol, G. Vergnaud, *Microbiology* **151**, 653 (2005).
4. A. Bolotin, B. Quinquis, A. Sorokin, S. D. Ehrlich, *Microbiology* **151**, 2551 (2005).
5. J. S. Godde, A. Bickerton, *J. Mol. Evol.* **62**, 718 (2006).
6. G. W. Tyson, J. F. Banfield, *Environ. Microbiol.* **10**, 200 (2008).
7. R. K. Lillestøl, P. Redder, R. A. Garrett, K. Brügger, *Archaea* **2**, 59 (2006).
8. R. Sorek, V. Kunin, P. Hugenholtz, *Nat. Rev. Microbiol.* **6**, 181 (2008).
9. P. Horvath *et al.*, *J. Bacteriol.* **190**, 1401 (2008).
10. H. Deveau *et al.*, *J. Bacteriol.* **190**, 1390 (2008).
11. R. Jansen, J. D. Embden, W. Gaastra, L. M. Schouls, *Mol. Microbiol.* **43**, 1565 (2002).
12. D. H. Haft, J. Selengut, E. F. Mongodin, K. E. Nelson, *PLoS Comput. Biol.* **1**, e60 (2005).
13. K. S. Makarova, N. V. Grishin, S. A. Shabalina, Y. I. Wolf, E. V. Koonin, *Biol. Direct* **1**, 7 (2006).
14. N. Beloglazova *et al.*, *J. Biol. Chem.*, **283**, 20361 (2008).
15. Materials and methods are available as supporting material on *Science* Online.
16. T. Baba, H. Mori, *Methods Mol. Biol.* **416**, 171 (2008).
17. T. H. Tang *et al.*, *Proc. Natl. Acad. Sci. U.S.A.* **99**, 7536 (2002).
18. T. H. Tang *et al.*, *Mol. Microbiol.* **55**, 469 (2005).
19. J. F. Kim, H. Jeong, R. E. Lenski, personal communication.
20. V. Kunin, R. Sorek, P. Hugenholtz, *Genome Biol.* **8**, R61 (2007).
21. A. Ebihara *et al.*, *Protein Sci.* **15**, 1494 (2006).
22. We thank T. Verweij, C. G. J. van Houte, and M. R. Beijer for experimental contributions and T. Goosen (Hogeschool van Arnhem en Nijmegen BioCentre), M. J. Young (Montana State University), T. Bisseling, and W. M. de Vos

Fig. 4. Engineered CRISPRs confer resistance to λ in the presence of Cascade and Cas3. (**A**) Effect of the presence of different sets of *cas* genes on the sensitivity of *E. coli* to phage λ_{vir}. Cells were equipped with one of two engineered CRISPRs containing four anti-λ spacers each (fig. S3). The C_{1-4} CRISPR produces crRNA complementary to the coding strand and mRNA of λ_{vir}, and the T_{1-4} CRISPR targets only the template strand. The sensitivity of each strain to phage λ_{vir} is represented as a histogram of the efficiency of plaquing, which is the plaque count ratio of the anti-λ CRISPR to that of the nontargeting control CRISPR. (**B**) Effect of single anti-λ spacers (fig. S3) on the sensitivity of *E. coli* to λ_{vir}. Error bars indicate 1 SD.

Suppression of the MicroRNA Pathway by Bacterial Effector Proteins

Lionel Navarro,[1] Florence Jay,[1] Kinya Nomura,[2] Sheng Yang He,[2] Olivier Voinnet[1]*

Plants and animals sense pathogen-associated molecular patterns (PAMPs) and in turn differentially regulate a subset of microRNAs (miRNAs). However, the extent to which the miRNA pathway contributes to innate immunity remains unknown. Here, we show that miRNA-deficient mutants of *Arabidopsis* partly restore growth of a type III secretion-defective mutant of *Pseudomonas syringae*. These mutants also sustained growth of nonpathogenic *Pseudomonas fluorescens* and *Escherichia coli* strains, implicating miRNAs as key components of plant basal defense. Accordingly, we have identified *P. syringae* effectors that suppress transcriptional activation of some PAMP-responsive miRNAs or miRNA biogenesis, stability, or activity. These results provide evidence that, like viruses, bacteria have evolved to suppress RNA silencing to cause disease.

In RNA silencing, double-stranded RNA (dsRNA) is processed into small RNAs (sRNAs) through the action of RNase-III–like Dicer enzymes. The sRNAs guide Argonaute (AGO)–containing RNA-induced silencing complexes (RISCs) to inhibit gene expression at the transcriptional or posttranscriptional levels (*1*). In the *Arabidopsis thaliana* microRNA (miRNA) pathway, miRNA precursors (pre-miRNAs) are excised from noncoding primary transcripts (pri-miRNAs) and processed into mature miRNA duplexes by Dicer-like 1 (DCL1). Upon HEN1-catalyzed 2′-O-methylation (*2*), one miRNA strand incorporates an AGO1-containing RISC to direct endonucleolytic cleavage or translational repression of target transcripts (*1*). DCL4 and DCL2 perform major defensive functions by processing viral-derived dsRNA into small interfering RNAs (siRNAs), which, like miRNAs, are loaded into AGO1-RISC. As a counterdefensive strategy, viruses deploy viral suppressors of RNA silencing, or VSRs (*3*). RNA silencing also contributes to resistance against bacterial pathogens (*4–7*), which elicit an innate immune response upon perception of pathogen-associated molecular patterns (PAMPs) by host-encoded pattern recognition receptors (PRRs). For example, the *Arabidopsis* miR393 is PAMP-responsive (*4*, *8*) and contributes to resistance against virulent *Pseudomonas syringae* pv. *tomato* strain DC3000 (*Pto* DC3000) (*4*). Nonetheless, the full extent to which cellular sRNAs, including miRNAs, participate in PAMP-triggered immunity (PTI) in plants remains unknown.

To address this issue, *Arabidopsis* mutants defective for siRNA or miRNA accumulation were challenged with *Pto* DC3000 *hrcC⁻*, a mutant that lacks a functional type III secretion system required for effector-protein delivery into host cells (*9*). This bacterium elicits but cannot suppress PTI and, consequently, multiplies poorly on wild-type Col-0– and La-*er*–inoculated leaves (Fig. 1A and fig. S1). However, *Pto* DC3000 *hrcC⁻* growth was specifically enhanced in the miRNA-deficient *dcl1-9* and *hen1-1* mutants (Fig. 1A), in which induction of the basal defense marker gene *WRKY30* was also compromised (fig. S2A) (*10*).

Because PTI is also a major component of nonhost resistance (*10*, *11*), we challenged *dcl1-9* and *hen1-1* mutants with *P. syringae* pv. *phaseolicola* (*Psp*) strain NPS3121, which infects beans but not *Arabidopsis*. Both *dcl1-9* and *hen1-1* mutants sustained *Psp* NPS3121 growth (Fig. 1B) and displayed compromised *WRKY30* induction (fig. S2B). Enhanced bacterial growth was also observed with the non-pathogenic *Pseudomonas fluorescens* Pf-5 and *Escherichia coli* W3110 strains (Fig. 1, C and D). Furthermore, the above nonvirulent bacteria all induced chlorosis and necrosis on miRNA-deficient mutants, resembling bacterial disease

[1]Institut de Biologie Moléculaire des Plantes, CNRS UPR 2353–Université Louis Pasteur, 12 Rue du Général Zimmer, 67084 Strasbourg Cedex, France. [2]Department of Energy Plant Research Laboratory, Michigan State University, East Lansing, MI 48824, USA.

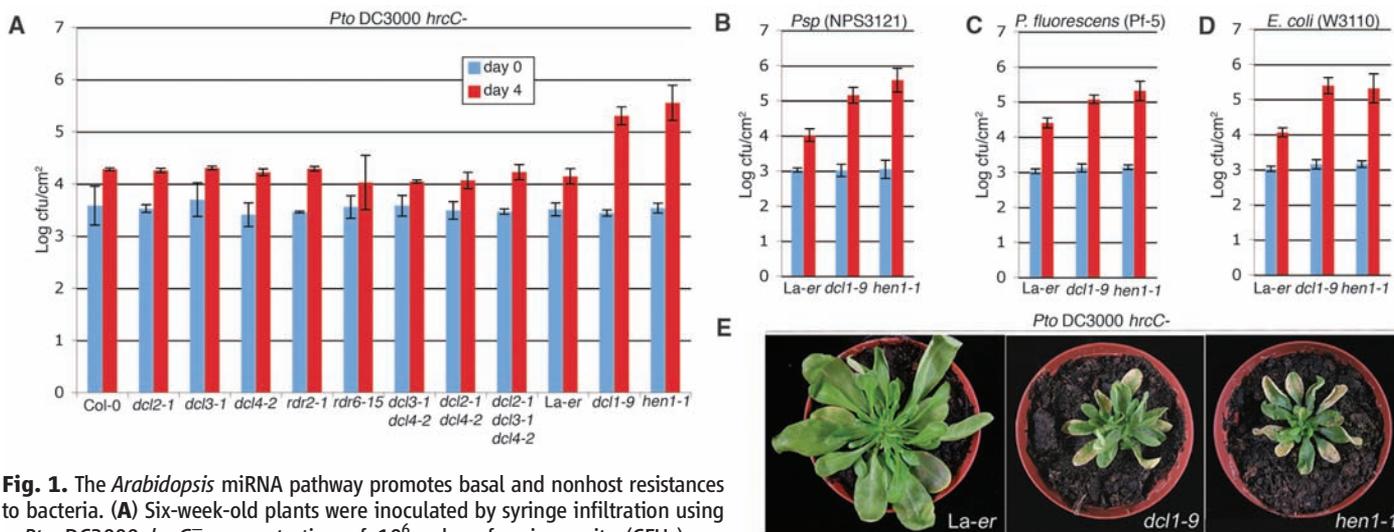*To whom correspondence should be addressed. E-mail: olivier.voinnet@ibmp-ulp.u-strasbg.fr

Fig. 1. The *Arabidopsis* miRNA pathway promotes basal and nonhost resistances to bacteria. (**A**) Six-week-old plants were inoculated by syringe infiltration using a *Pto* DC3000 *hrcC⁻* concentration of 10^6 colony-forming units (CFUs) per milliliter. Error bars indicate SE of log-transformed data from five independent samples. Similar results were obtained in three independent experiments. (**B** to **D**) Plants were inoculated as in (A) but with *Psp* NPS3121 (B), *P. fluorescens* Pf-5 (C), or *E. coli* W3110 (D). Similar results were obtained in two independent experiments. (**E**) Plants were inoculated as in (A) and pictures were taken at 6 days after inoculation.